Lifetime-oriented modelling of vortex-induced across-wind vibrations on bridge tie rods

M. Gálffy, A. Wellmann Jelic & D. Hartmann
Institute of Computational Engineering, Faculty of Civil Engineering, Ruhr-University Bochum, Germany
galffy@inf.bi.rub.de, andres.wellmann@rub.de, hartus@inf.bi.ruhr-uni-bochum.de

Summary

The influence of vortex-induced vibrations on vertical tie rods has been proved as a determinant load factor in the lifetime-oriented dimensioning of arched steel bridges. Particularly, the welded connection plates between the suspenders and the arches often exhibit cracks induced primarily by high-cycle fatigue, as a consequence of the vortex-induced across-wind vibrations of the tie rods. In this context, the synchronization of the vortex-shedding to the rod motion in a critical wind velocity range, the so-called *lock-in* effect, is of essential interest.

The model proposed in (Ruscheweyh 1982) describes the aeroelastic effects only in a smooth flow. In (Vickery, Clark 1972), a theoretical approach for the turbulent flow is presented, but without consideration of the *lock-in* effect. Models for the *lock-in* effect in a turbulent flow have been proposed in (Vickery, Basu 1983) and in (ESDU 1996).

This contribution presents a wind load model, based on the convolution integral developed in (Lou 1997), improved by considering time dependent wind velocities and including the *lock-in* effect. This model has been validated by wind tunnel measurements and by full scale experiments on an arched bridge.

The stresses caused by the vibrations are computed on a finite element model, according to the structural stress concept. The expected lifetime within the limit of the 97.5 % fractiles is estimated from the accumulated damage, according to the Palmgren-Miner rule, the stress-cycles are counted by the rainflow method.

1 Introduction

This work is part of the project C5 of the Collaborative Research Center (SFB) 398, dealing with the lifetime-oriented optimization of structures, under the consideration of fatigue. In this context, the focus lies on the analysis of the vertical tie rods of arched steel bridges, because the welded plates, which connect the rods with the arches, are extremely damage-sensitive. The structure-design must be based on a precise knowledge of the time variant structural response and on a precise prediction of the induced deteriorations. Therefore, the loadings have to be modeled as realistically as possible, according to their stochastic nature.

The influence of vortex-induced across-wind vibrations is a dominant load factor causing the damage process. These vibrations occur, when vortices are alternately shed from opposite sides of the rods, creating forces in across-wind direction. In a smooth flow, these loads alternate harmonically, with the Strouhal-frequency f_s, which is proportional to the wind velocity u:

$$f_s = \frac{S u}{D} \tag{1}$$

(S and D are the Strouhal-number and the rod-diameter, respectively). In a turbulent flow, the excitation frequencies are distributed in an interval around the mean frequency, the width of the interval increasing with the turbulence.

The synchronization of the vortex shedding to the system motion, for wind velocities within a critical range — called the *lock-in* effect — plays an essential role in the excitation process.

Since neither the model proposed in (Ruscheweyh 1982), nor that in (Vickery, Clark 1972) predicts the magnitude of the across-wind oscillation amplitude of the bridge tie rods as experimentally measured, in the project C5 a wind load model has been developed, which estimates the amplitude accurately. The changes in the nature of the excitation-force caused by entering or exiting the *lock-in* range lead to an excitation process that is basicly non-stationary. As a consequence, the load model used should describe the excitation force also in a non-stationary flow.

2 Outline of the model for across wind vibrations in turbulent flow

In (Lou 1997), the lift force per unit length w acting on a cylinder due to vortex shedding in a stationary turbulent flow, outside of the *lock-in* wind velocity range, is given in terms of a convolution integral:

$$w(t) = \frac{\rho}{2}\beta D C_l \int_0^t u^2(\tau)\, e^{-\bar{\xi}(t-\tau)} \cos\bar{\omega}(t-\tau)\,\mathrm{d}\tau. \tag{2}$$

In equation (2), ρ is the density of air, C_l is the lift coefficient, $u(\tau)$ is the fluctuating wind velocity, and $\bar{\omega} = 2\pi S\bar{u}/D$ is the mean Strouhal angular frequency being proportional to the stationary mean wind velocity $\bar{u}$.

The integral (2) is based on the assumption of a Gauss-distributed spectral density of the lift force, as described in (Vickery, Clark 1972). Based on this assumption, the parameter $\bar{\xi}$ can be determined as

$$\bar{\xi} = \sqrt{\ln 4}\, I_u \bar{\omega}, \tag{3}$$

where I_u is the wind-turbulence. From the spectral density assumption, also the parameter β can be explicitely evaluated, but for the present model a power-function dependence of β on the wind velocity u is favored: $\beta = K u^{n-2}$, where K and n are fit-parameters. In order to describe the non-stationary wind process, the mean values in (2) are replaced by the corresponding time-dependent quantities. Only the wind turbulence I_u is supposed to be constant. The lift force per unit length w acts over the correlation length L_c, which is the length-scale of the synchronized vortex shedding. As a first estimation, the correlation length has been set to $L_c = 6D$, according to (Ruscheweyh 1982).

The resulting force acting on the rod is then obtained as:

$$F(t) = \frac{\rho}{2} K D C_l L_c \int_0^t u^n(\tau)\, e^{\alpha(t,\tau)} \cos\varphi(t,\tau)\,\mathrm{d}\tau, \tag{4}$$

where

$$\alpha(t,\tau) = \int_t^\tau \xi(x)\,\mathrm{d}x, \qquad \varphi(t,\tau) = \int_t^\tau \omega(x)\,\mathrm{d}x + \varphi_0(t), \tag{5}$$

$$\xi(x) = \sqrt{\ln 4}\, I_u \omega(x), \qquad \omega(x) = \frac{2\pi S}{D} u(x). \tag{6}$$

The value of the integral (4) is in fact determined only by the history of the wind-velocity in a certain time interval preceeding t. Wind-events dating further back are suppressed due to the exponentially decaying factor $e^{\alpha(t,\tau)}$.

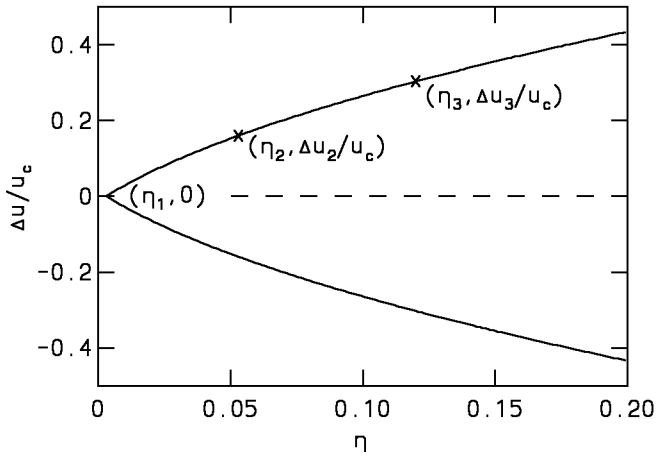

Figure 1: Width of the *lock-in* range for bridge tie rods

The parameter φ_0 in (5) describes the *lock-in* effect. For wind velocities in the *lock-in* range, it is set in phase with the rod motion according to

$$\varphi_0(t) = \pi + \arctan \frac{v(t)}{\omega_0 y(t)}. \tag{7}$$

Outside of the *lock-in* range, $\varphi_0(t)$ equals 0. The quantity ω_0 is the angular eigenfrequency of the rod, $v(t)$ and $y(t)$ are the velocity and the displacement of the rod at the time t.

The excitation force $F(t)$ is applied at a single point, at the rod-section exhibiting the maximal amplitude, the values $v(t)$ and $y(t)$ also referring to this section. Because the phase-synchronization leads to an increase of the rms-amplitude of the force, the multiplicative parameter K in (4) is reduced for the *lock-in* range, to compensate the increase.

The *lock-in* range is defined as a range around the critical wind velocity $u_c = f_0 D/S$ (f_0 is the eigenfrequency of the rod), with a half width $\Delta u = |\bar{u} - u_c|$ depending on the relative vibration amplitude $\eta = 2A/D$ (A is the vibration amplitude). A simple parabolic dependence of the relative band-width $\Delta u/u_c$ on η is assumed, defined by three points $(\eta_1, 0)$, $(\eta_2, \Delta u_2/u_c)$ and $(\eta_3, \Delta u_3/u_c)$, as shown in figure 1. The points are obtained from fits to the experimental data. The assumed *lock-in* range is symmetric for wind velocities below and above the critical value.

Note, that the mean wind velocity is only used in the model for the purpose of the determination of the *lock-in* range.

3 Validation of the wind load model by full scale experiments on an arched bridge in Münster-Hiltrup

The load model has been validated by wind tunnel measurements (Gálffy et al. 2004) and by full scale experiments carried out on an arched bridge in Münster-Hiltrup. For this purpose, a realistic finite element model of the oscillating system has been generated. The model has been excited with a force, that resulted from the convolution integral (4) applied to the measured wind-data $u(\tau)$. The calculation of the displacements has been performed in the time domain, using the well-known Newmark-Wilson time-step method.

The arched steel bridge in Münster-Hiltrup is provided with tie rods of 5 different lengths, denoted as type 1–5. All of them have a circular cross-section of the diameter $D = 110\,\text{mm}$. The suspenders are fixed by welded steel plates (1.1 m high, maximal width 1.1 m, thickness $d = 25\,\text{mm}$),

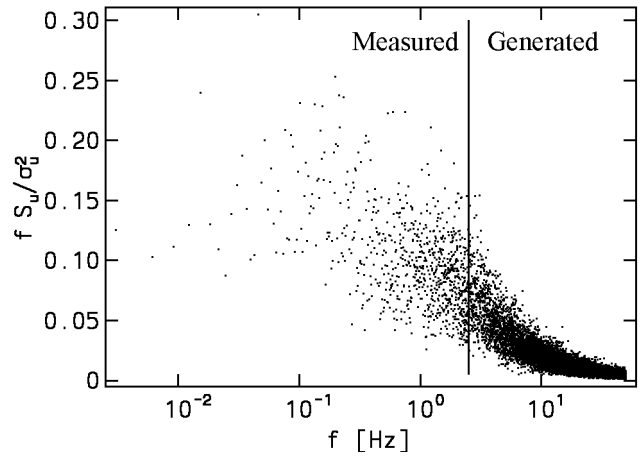

Figure 2: Spectrum of the reconditioned wind data (1st measurement)

which are oriented parallel to the bridge girder at the girder-connection and perpendicular to the bridge girder at the arch-connection. Two neighboured tie rods — of type 4 and 5 — have been selected for the measurement. The entire lengths of the suspenders, including the plates, are 10.4 m (type 4) and 11.1 m (type 5). For both rod types, the tension force under self-weight amounts to 780 kN. The logarithmic damping decrement has been evaluated to $\delta = 0.0005$ (type 4) and $\delta = 0.0007$ (type 5), providing the Scruton-numbers $Sc = 4.9$ and $Sc = 6.9$.

The vibration of the tie rods has been monitored by two digital cameras mounted on tripods placed on the sidewalk and fixed on the section of the rods showing the maximal vibration amplitude. Since the main wind direction was perpendicular to the bridge girder, the cameras have been placed in such a way that they could detect the rod motions along the bridge axis, i. e. in across-wind direction. An ultrasonic 3D-anemometer has been placed between the two rods, which measured the oncoming wind, along with a sensor that detected the girder acceleration. From the incoming wind data, only the horizontal velocity component along the river has been used for the simulation. The sampling rate of the wind and acceleration data was 100 Hz.

Two measurements have been performed: during the first one, both tie rods have been monitored for ca. 50 minutes, during the second one, only the type 4 rod has been recorded for ca. 20 minutes. Then, the digital videos have been analysed by a self-provided Java program to obtain the time-dependent displacements. The videos contain 25 frames per second, each of them consisting of two half-frames. Thus, the displacements have been obtained at a sampling rate of 50 Hz. The spatial resolution of the cameras was about 0.3 mm per pixel. Through averaging over the entire image height, the resolution could be increased to about 0.01 mm. The girder-acceleration and the low-frequency part ($f < 1$ Hz) of the deflection show peaks induced by the traffic on the bridge, occuring at the same time in both sets of data. As the acceleration has been recorded synchronously with the wind velocity, the acceleration data could be used to synchronize the wind and the deflection data, with an error less than ± 0.5 s.

Since the physical sampling rate of the ultrasonic anemometer was only 5 Hz, the original wind data contained useable data only in the range below the Nyquist-frequency $f_N = 5/2 = 2.5$ Hz. Therefore, the wind data have been reconditioned in such a way that the frequency part above 2.5 Hz has been replaced by stochastically generated data. Figure 2 shows the wind spectrum used for the simulation (here, σ_u is the standard deviation of the along-wind component of the velocity). The turbulence, as determined from both the original and the reconditioned wind data, was $I_u = 0.17$.

From the Fourier-spectra of the oscillations, the eigenfrequencies $f_0 = 7.88$ Hz (rod type 4) and

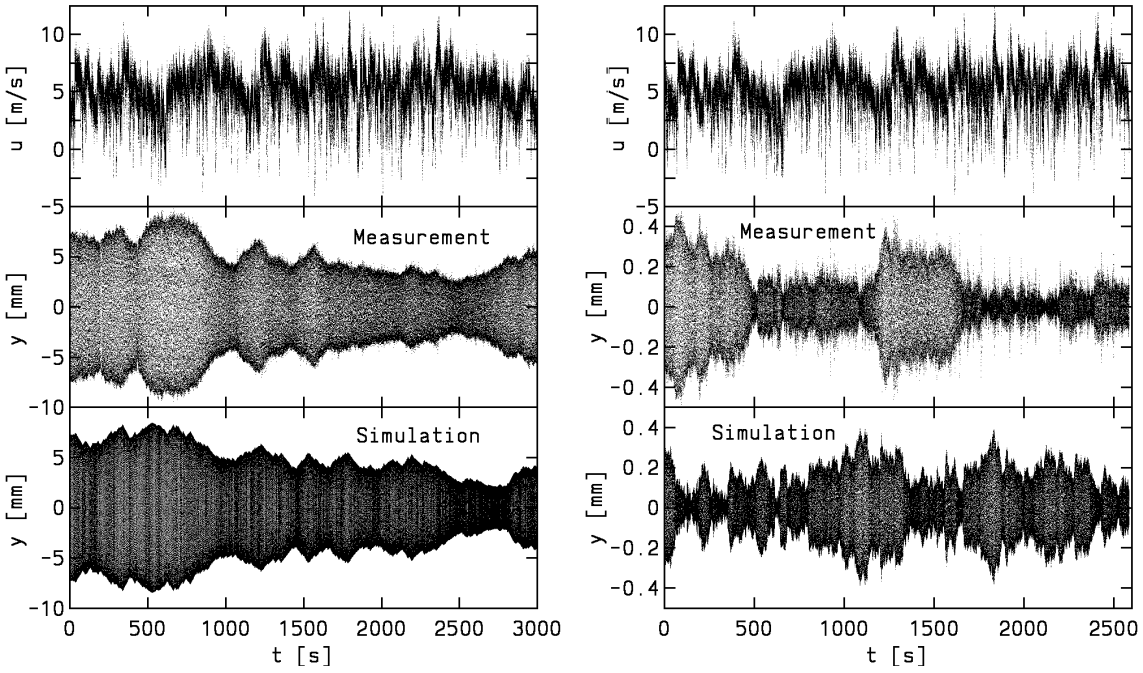

Figure 3: Wind velocity, measured and simulated deflection, 1st measurement, tie rod type 4 (left) and 5 (right)

$f_0 = 6.71$ Hz (rod type 5) have been evaluated, showing a good agreement with the results of the finite element analysis. For the simulation, a Strouhal-number $S = 0.22$ has been chosen as the value providing the best fit to the measured data. The Reynolds-number at the critical wind velocity $u_c = 3.94$ m/s (rod type 4) and $u_c = 3.36$ m/s (rod type 5), respectively, is $Re = 2.9 \cdot 10^4$ and $Re = 2.5 \cdot 10^4$, respectively, referring to the subcritical wind velocity range.

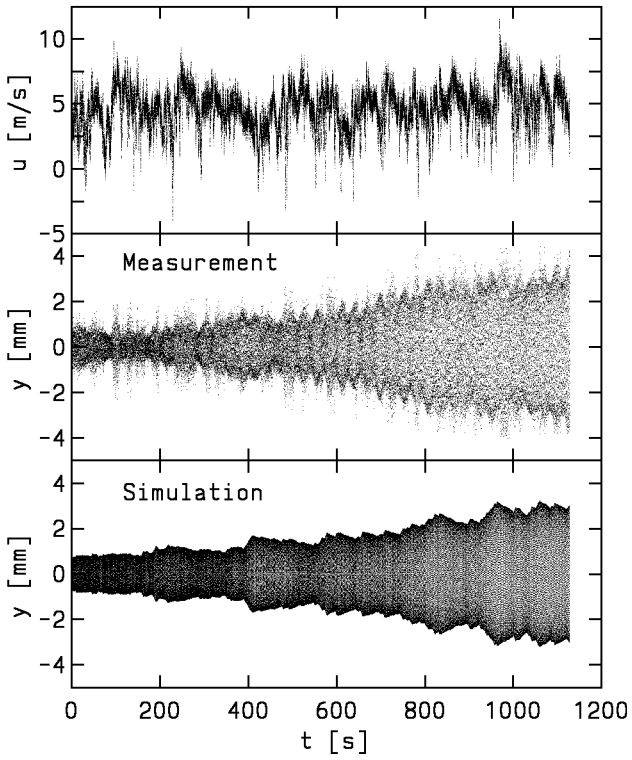

Figure 4: Wind velocity, measured and simulated deflection, 2nd measurement, tie rod type 4

Figures 3 and 4 present the wind velocity, the measured and the simulated rod-deflections as a function of time. It should be mentioned that the measured deflections presented in these figures have been obtained by cutting the low-frequency part ($f < 1$ Hz) of the original signal, using a Fourier-filter. In the computer-simulation, the parameters $K = 175\,\mathrm{m}^{-1}$ and $n = 3$ have been applied. For the *lock-in* range, which has been defined by the parameters $\eta_1 = 0.0035$, $\eta_2 = 0.053$, $\eta_3 = 0.12$, $\Delta u_2/u_c = 0.156$ and $\Delta u_3/u_c = 0.300$ (see figure 1), the parameter K has been reduced by the factor 4. The lift-coefficient, has been set to $C_l = 0.5$, according to (ESDU 1996), while the correlation length has been assumed as $L_c = 6D = 0.66\,\mathrm{m}$.

Table 1: Averaged rms-amplitudes [mm] of the measured and simulated deflections

1st measurement				2nd measurement	
rod type 4		rod type 5		rod type 4	
measured	simulated	measured	simulated	measured	simulated
3.81	3.81	0.133	0.130	1.32	1.32

Table 2: Time-ratios spent at *lock-in*

1st measurement		2nd measurement
rod type 4	rod type 5	rod type 4
39.3 %	0.2 %	19.6 %

Table 1 summarizes the averaged rms-amplitudes of the measured and simulated deflections. The time-ratios spent at *lock-in*, as determined from the simulation-runs, are listed in table 2.

As can be seen from figure 3 and 4, the measured averaged rms-amplitudes, as well as the time-dependence of the oscillation amplitude on entering or exiting the *lock-in* range, are satisfactorily approximated by the simulation.

In contrast to that, the Ruscheweyh-model (Ruscheweyh 1982) predicts for the type 4 rod a peak amplitude of about 5 mm in the *lock-in* range, while the model in (ESDU 1996) yields an rms-amplitude of ca. 30 mm. It can be stated that both models show a substantial discrepancy compared to the measured values: Approximately a 9 mm peak amplitude and an rms-amplitude of about 6 mm have been determined for the time-interval between 500–800 s (see figure 3).

4 Application in lifetime oriented design

The high-cycle loading caused by the vortex-induced vibrations primarily induces cracks in the welded connection plates that link the vertical suspenders with the bridge arches. Unsuitable plate geometries, having high stress peaks, accelerate the initiaton of these cracks. Accordingly, such layouts are critical with respect to the lifetime-oriented design of the connecting plates and the structure in total. A shape optimization of the plates, therefore, is desirable, taking into consideration the stochastic time-dependent fatigue history.

4.1 Generation of the stochastic wind data

In a first step, several realizations of stochastic time processes, representing the wind velocity at the half height of the correspondent vertical tie rod, have been generated. For that, white noise has

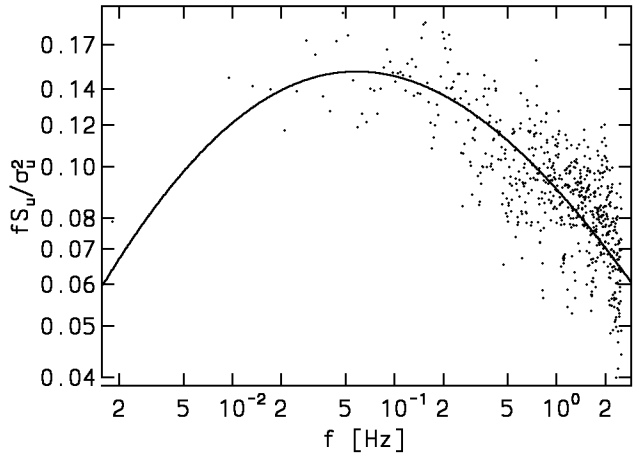

Figure 5: Measured wind velocity spectrum (dots) and fitted Fichtl-McVehil spectrum (solid line)

been transformed into a Gaussian process, and then, to a wind process using the inverse discrete Fourier-transform (FFT), in order to obtain a Fichtl-McVehil spectral density. The Fichtl-McVehil spectrum is defined as

$$\frac{fS_u(f)}{\sigma_u^2} = \frac{a\frac{fL_{ux}}{\bar{u}}}{\left[1+b\left(\frac{fL_{ux}}{\bar{u}}\right)^r\right]^{\frac{5}{3r}}}, \tag{8}$$

where $S_u(f)$ is the wind spectral density at the frequency f, while $\bar{u}$ and σ_u are the mean value and the standard deviation of the wind velocity u. The quantity L_{ux} is the integral length of the turbulent wind, a, b and r are fit-parameters.

From the low-frequency part of the measured wind data ($f \leq 2.5\,\text{Hz}$), the following parameter values have been esimated (see figure 5): $L_{ux} \approx 60\,\text{m}$, $a \approx 17$, $b \approx 1.7$, $r \approx 0.35$. Finally, the values have been shifted and scaled to obtain the required mean value and standard deviation. For all runs, the standard deviation has been taken proportional to the mean wind velocity, the latter representing the only free parameter in the definition of the stochastic wind data.

The weak damping and the large mass of the rods lead to slow answers of the system due to changes of the excitation force — e. g. due to entering or exiting the *lock-in* range. Therefore, larger durations are selected for these time processes. As the FFT requires that the number of data is an integer power of 2, if 0.01 s is chosen for the time-step of the Newmark-Wilson method, a suitable duration is $t = 0.01 \cdot 2^{19} = 5242.88\,\text{s} \approx 1.5$ hours.

The stochastically generated time-dependent wind velocities described above have been used as input for the convolution model introduced in section 2, for computing the correspondent lift forces on the tie rod orthogonal to the mean wind direction, and the time-histories of the deflections by virtue of the Newmark-Wilson time-step method.

4.2 Calculation of the local stresses

The local stresses in the connection plate have been computed according to the structural stress concept. For that, a realistic finite element model of the type 4 tie rod of the Münster-Hiltrup bridge, including its two connection plates, has been generated. For the dominant load case — i.e. wind velocity perpendicular to the girder, hanger oscillations parallel to the girder — the connection plates are exposed to in-plain strain at the bridge girder and to bending at the arch. Because the bending stiffness of the bridge girder is much higher than that of the tie rod, the edge

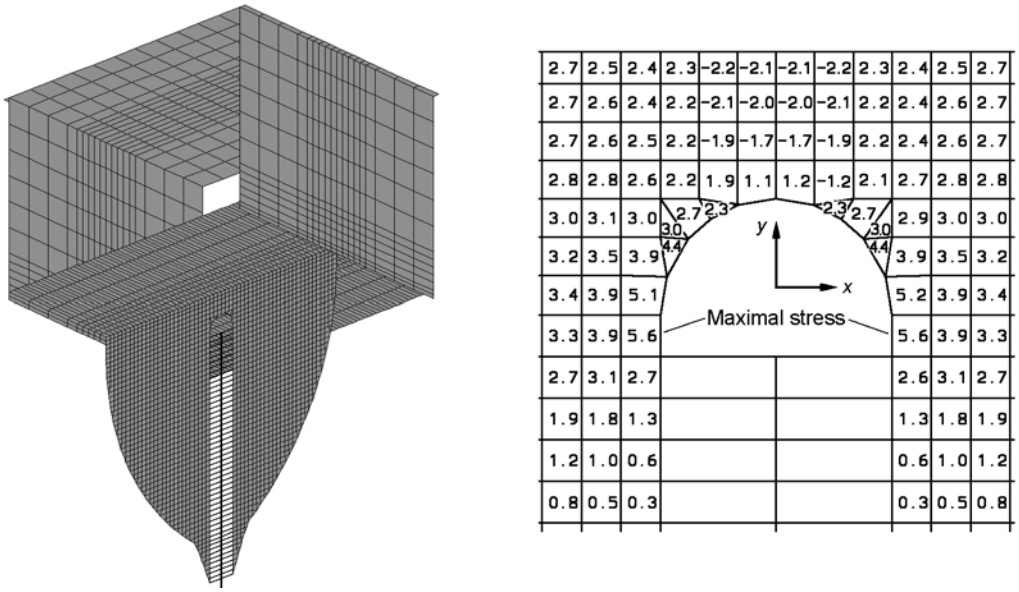

Figure 6: Left: finite element model of the connection plate, right: stresses σ_y [N/mm^2] in the critical region, caused by a rod deflection of 1 mm

of the plate welded to the girder profile has been defined as a clamped support. On the upper end of the system, a 1 m portion of the bridge arch has been generated (see figure 6, left part), in order to correctly represent the clamping conditions of the plate edge welded to the arch profile.

For this system, the eigenshape for the lowest eigenfrequency has been determined. In the stiffness-matrix of the system, also the geometric stiffness of all bars and shell elements resulting from the 780 kN tension force under self-weight has been taken into consideration. Based on the computed deformation, scaled to a deflection-amplitude of 1 mm, the corresponding stresses in the shell elements have been calculated. It turned out that the maximal stress caused by bending in the arch connection plate becomes $\sigma_y = 5.6\,\text{N/mm}^2$, occuring in the elements shown in the right part of figure 6. The determined values refer to the midsts of the elements, i. e. to points about $1.4\,\text{cm} = 0.56\,d$ distant from the re-entrant corner of the plate (d is the thickness of the plate). In the girder connection plate, the maximal stresses caused by in-plane strain are only about $\max\sigma = 4.0\,\text{N/mm}^2$.

4.3 Calculation of the partial damages

Using the maximal stress $\sigma_y = 5.6\,\text{N/mm}^2$ per 1 mm deflection as a stress factor, the stress time histories at the maximum stress point have been computed. As known, besides the mean wind velocity $\bar{u}$ also the initial oscillation amplitude of the rod A_0 plays a critical role with respect to the evolution of the stress time history. Therefore, stress time histories have been created for 22 different values $\bar{u}$, with $1.0\,\text{m/s} < \bar{u} < 10.0\,\text{m/s}$, along with 11 different values for A_0, $0 < A_0 < 10\,\text{mm}$ for each $\bar{u}$. As the stress time histories considerably vary between the different, stochastically equivalent realizatons (i.e. realizations differing only in the initialization value of the random number generator creating the white noise), 50 realizations for each parameter-pair $(\bar{u}, A_0)$ have been generated in order to obtain a feasible statistical distribution.

From the stress time histories, the histograms of cycles have been established using the rainflow cycle counting method, and then, the partial damage has been computed for each realization (duration $\Delta t = 5242.88\,\text{s}$) according to the Palmgren-Miner accumulation rule, using the Woehler curves given in Eurocode 3 for bulk steel: notch class 160, fatigue strengths $\sigma_D = 117\,\text{N/mm}^2$ and

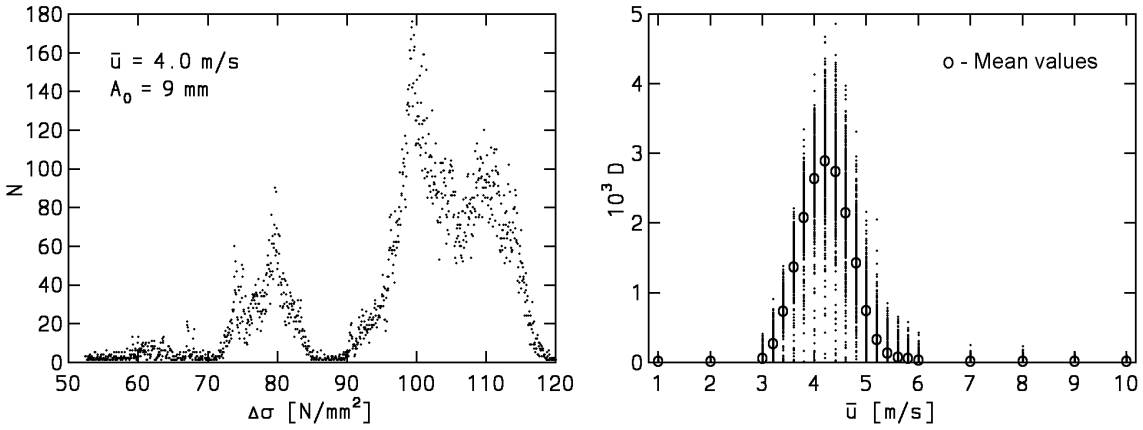

Figure 7: Left: histogram of cycles obtained by the rainflow method, right: partial damages vs. mean wind velocity

$\sigma_L = 64\,\mathrm{N/mm^2}$, representing the 97.5 % fractile.

Figure 7 presents a typical histogram of cycles, containing the number of cycles N plotted against the double stress amplitude $\Delta\sigma$ and the computed partial damages D as a function of the mean wind velocity $\bar{u}$.

In a last step of the validation of our wind load model, also the damage resulting from deflections simulated, using the measured (reconditioned) wind data has been checked against the results obtained from measured deflections (see figure 3–4). The damage resulting from measured deflections of the rod type 4 in the 1st measurement is $D = 2.35 \cdot 10^{-4}$. From simulated deflections $D = 2.42 \cdot 10^{-4}$ is obtained. Consequently, the two values show a respectable agreement. For the rod type 5 and in the 2nd measurement of the rod type 4, the stresses are below $\sigma_L = 64\,\mathrm{N/mm^2}$ and therefore no damage occurs.

Finally, an assessment of the damage accumulated at the critical region of the connection plate in a period of one year has been conducted. The distribution of the mean wind velocity for one year, has been published by the German Meteorological Service (Deutscher Wetterdienst) (Christoffer 1989). The data for the meteorological station in Bockholt have been used, as they are representative for the Münster region. The distribution is given by the Weibull function:

$$F(\bar{u}) = 1 - e^{-\left(\frac{\bar{u}}{a}\right)^k} \tag{9}$$

and the corresponding probability density

$$f(\bar{u}) = \frac{k}{a}\left(\frac{\bar{u}}{a}\right)^{k-1} e^{-\left(\frac{\bar{u}}{a}\right)^k}, \tag{10}$$

where a and k are the scale and shape parameters.

The scale and shape parameters depend on the wind direction. 12 values a_i and k_i are available, corresponding to sectors of 30°. The across-wind tie rod vibrations are only caused by the component of the wind velocity perpendicular to the bridge axis. The distribution function for this component can be assumed as follows:

$$F(\bar{u}) = \sum_{i=1}^{12} \left[1 - e^{-\left(\frac{\bar{u}}{a_i |\sin \alpha_i|}\right)^{k_i}} \right]. \tag{11}$$

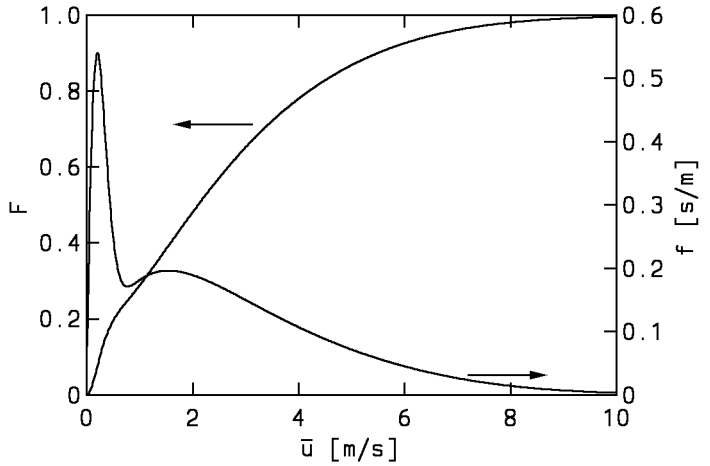

Figure 8: Probability function (left scale) and probability density (right scale) of the mean wind velocity component perpendicular to the bridge axis

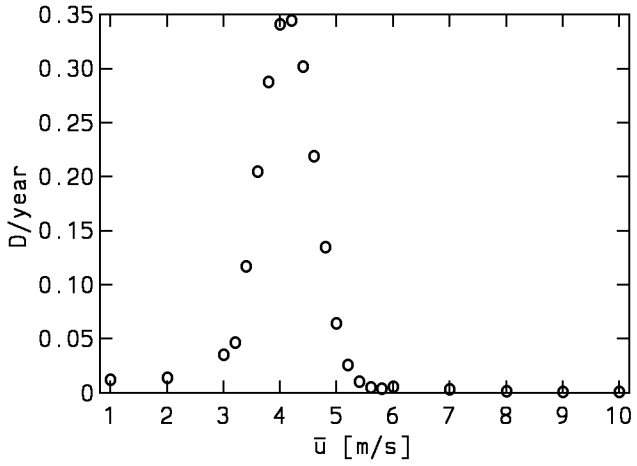

Figure 9: Damage accumulated during one year vs. mean wind velocity

Here, α_i is the angle between the bridge axis and the bisector of the i-th wind direction sector. Figure 8 shows the obtained distribution function and the corresponding probability density.

As a year corresponds to 6019 time intervals $\Delta t = 5242.88$ s, the number of time intervals Δt per year having mean wind velocities in the interval $[\bar{u}_1, \bar{u}_2)$ evaluates to

$$N_{\Delta t} = 6019\,(F(\bar{u}_2) - F(\bar{u}_1)). \tag{12}$$

Setting $\bar{u}_1 = (\bar{u}_{j-1} + \bar{u}_j)/2$ and $\bar{u}_2 = (\bar{u}_j + \bar{u}_{j+1})/2$, $N_{\Delta t}(\bar{u}_j)$ is evaluated for each of the 22 mean wind velocity values $\bar{u}_j$ used in the stochastic data generation. Multiplying $N_{\Delta t}(\bar{u}_j)$ with the calculated average partial damage for one simulation period Δt (circles in figure 7, right part), the damage accumulated during a 1 year period is obtained for the specified mean wind velocity range. This damage is plotted in figure 9 as a function of the mean wind velocity. As a first estimation of the total damage accumulated in the connection plate over the period of 1 year, $D \approx 2.2$ has been determined from the sum of the damages for all mean wind velocity ranges.

4.4 Discussion of the results

The first estimation yealds a damage accumulation of $D \approx 2.2$ in the connection plate due to vortex-induced across-wind vibrations, with respect to a 1 year period. Since the Woehler-curve in

the Eurocode 3 relies on the 97.5 % fractiles, this result may be misinterpreted as a $P_f = 2.5 \cdot 10^{-2}$ failure probability for the connection plate corresponding to a lifetime of about only half a year.

However, it is believed that this result does not mean that visible damages in the plate will occur after this short time. The reason for this is that the Woehler-curve in the Eurocode 3 is extremely restrictive compared to other codes concerning fatigue. First, the Eurocode does not distinguish between steel grades, and second, the mean stress value (e. g. due to dead load) is included in the Woehler-curve safety concept and can be ignored in the static proof.

In order to elucidate the differences, a check of the weld between the plate and the hanger is presented, according to the German Code for Crane-Beams and Steel Structures, DIN 4132. The grade of the steel used is St 52, the notch class of the weld is K0. The tensile stress resulting from the dead load (tension-force $N = 780$ kN) is $113\,\mathrm{N/mm^2}$, the alternating stress resulting from a tie rod vibration having an assumed maximal amplitude of 10 mm is $\pm 56\,\mathrm{N/mm^2}$. Then the resulting upper and lower stress values are $\sigma_u = +169\,\mathrm{N/mm^2}$ and $\sigma_l = +57\,\mathrm{N/mm^2}$, leading to a stress ratio of $\kappa = +0.34$. According to the stress ratio $\kappa = +0.3$ and the highest stressing group B6, the above mentioned DIN 4132 allows a maximal upper stress of $173.3\,\mathrm{N/mm^2} > \sigma_u = 169\,\mathrm{N/mm^2}$, i. e., the stress in the weld is admissible. As the admissible stresses for the bulk material are higher than for welds, the proof also holds for the plate itself.

5 Conclusions and outlook

Based on validation-experiments, along with numerical simulations, an adequate load model has been found, by which the vortex-induced across-wind vibrations of the vertical tie rod of arched steel bridges can be sufficiently represented. The established load model has been used for a first estimation of the lifetime of the welded hanger connection plates. The theoretically computed, unexpectedly short lifetime of about 1/2 year, evaluated on the basis of the Woehler-curve in Eurocode 3 turns out to be not realistic. Therefore, in a further step of the investigations, more appropriate Woehler-curves are to be considered.

Furthermore, it is intended to introduce structure-oriented, stochastically defined Woehler-curves instead of curves based on the fractile-concept, and simultaneously the *masing* and *memory* effects in the rainflow method are to be implemented for counting the stress cycles. Also, it is a matter of ongoing investigation to consider the dependence of the computed damage on the initial vibration amplitude according to its stochastic nature, with regard to the considerable scattering of the values (i. e. the large differences between the realizations).

The improvements mentioned above are then incorporated into the design optimization process that is the main issue in the C5 project and materialized in terms of a software system.

Acknowledgements

We thank R. Höffer and J. Sahlmen (Aerodynamics Institute of the Ruhr-University Bochum) for useful discussions. We also appreciate the assistance of J. Rauter and R. Elke (members of the same institute) in installing the measuring equipement for the full-scale measurements.

Thanks are also due to the Deutsche Forschungsgemeinschaft which facilitates the research-work through the SFB 398 funds.

References

Christoffer, H. and Ulbricht-Eissing, M. (1989). *Die bodennahen Windverhältnisse in der Bundesrepublik Deutschland.* Berichte des Deutschen Wetterdienstes 147. Selbstverlag des Deutschen Wetterdienstes.

ESDU (1996). *Response of structures to vortex shedding. Structures of circular or polygonal cross section.* Item No. 96030, ESDU International, London.

Gálffy, M., Wellmann, A., Hartmann, D. (2004). Modelling of vortex-induced across-wind vibrations on bridge tie rods. *Lifetime-Oriented Design Concepts, 2nd International Conference, Bochum*: 421–429

Lou, J. (1997). Quasi-stationäre Modellierung und numerische Simulation der Wind-Wechselwirkung an zylindrischen Bauwerken. *Technical Reports*, 97-3: 11–15. Institut für Konstruktiven Ingenieurbau, Ruhr-Universität Bochum

Ruscheweyh, H. (1982) *Dynamische Windwirkungen an Bauwerken.* Bauverlag GmbH Wiesbaden Berlin.

Vickery, B. J., Clark, A. W. (1972). Lift or across-wind response of tapered stacks. *Journal of the Structural Division (ASCE)* 98: 1–20.

Vickery, B. J., Basu, R. J. (1983). Simplified approaches to the evaluation of the across-wind response of chimneys. *Proc. 6th Int. Conf. on Wind Engineering*, Gold Coast, Australia, *J. Wind Eng. Ind. Aerodyn.* 14: 153–166